THE ASTROPHYSICAL JOURNAL, 259:647–656, 1982 August 15

FAR-INFRARED ROTATIONAL EMISSION BY CARBON MONOXIDE

CHRISTOPHER F. MCKEE,[1] J. W. V. STOREY, AND DAN M. WATSON
Department of Physics, University of California, Berkeley
AND
SHELDON GREEN
NASA Institute for Space Studies
Received 1981 April 27; accepted 1982 February 9

ABSTRACT

Accurate theoretical collisional excitation rates are used to determine the emissivities of CO rotational lines for $n(H_2) \geq 10^4$ cm^{-3}, 100 K $< T <$ 3000 K, and $J \leq 60$ under the assumption that the lines are optically thin. An approximate analytic expression for the emissivities which is valid in this region is obtained. Population inversions in the lower rotational levels occur for densities $n(H_2) \approx 10^{3-5}$ cm^{-3} and temperatures $T \gtrsim 50$ K provided photon trapping is unimportant. Interstellar shocks observed edge-on are a potential source of weak millimeter-wave CO maser emission. The CO rotational cooling function suggested by Hollenbach and McKee is verified, although their numerical value is several times too large at low densities.

Subject headings: infrared: spectra — masers — molecular processes

I. INTRODUCTION

The development of far-infrared spectroscopy is opening a new window on the universe. Rotational lines of astronomically abundant molecules often lie in the far-infrared. Observation of these lines provides a powerful probe for determining both the density and temperature of the emitting gas, as recently demonstrated by the interpretation of the observations of the $J = 21 \rightarrow 20$, $22 \rightarrow 21$, $27 \rightarrow 26$, and $30 \rightarrow 29$ lines of CO in Orion (Watson *et al.* 1980; Storey *et al.* 1981). Using collisional excitation cross sections calculated by one of us (S. G.), Storey *et al.* (1981) calculated the CO rotational level populations and line intensities for a number of temperatures and densities and showed that the observed intensities in Orion could be modeled by emission from two components: a 2000 K component with $n(H_2) \approx 1 \times 10^6$ cm^{-3} and a 400–1000 K component with $n(H_2) \approx 5\text{–}2 \times 10^6$ cm^{-3}.

Inverting a 51×51 matrix to determine the level populations (as done by Storey *et al.*) is somewhat cumbersome for interpreting data, and it is awkward for theoretical calculations of the emission spectra of shocks as well. In this paper accurate numerical results for the line intensities for optically thin CO collisionally excited by H_2 are presented for a number of points in the regime $n(H_2) \geq 10^4$ cm^{-3} and 100 K $\leq T \leq$ 2000 K (§ II). In § III we use an approximation introduced by Hollenbach and McKee (1979; hereafter HM) to obtain an analytic expression for the level populations and line intensities which is accurate to within a factor of 1.3 over most of this regime. Since the theoretical collision cross sections have an accuracy of about 30% and astronomical observations average over regions at a variety of temperatures and densities, the analytic approximation should be quite adequate for astronomical purposes. Inversion of the lower rotational levels is discussed in § IV. We also use the numerical results to evaluate the accuracy of the CO cooling rate found by HM (§ V).

Although we have focused on CO as the typically most abundant molecule other than H_2, our methods should also apply directly to other linear molecules such as HCN, HC_3N, and HCO^+.

II. EXACT CALCULATION OF POPULATIONS

Calculation of the equilibrium population of each state requires first of all a detailed knowledge of the entire matrix of collisional rate coefficients, $\gamma_{JJ'}$, from every state, J, to every other state, J'. Although such detailed information cannot yet be obtained experimentally, it has been possible to obtain fairly accurate values theoretically. This involves two steps, computing the intermolecular forces and then calculating the scattering dynamics. In an early study, Green and Thaddeus (1976) obtained the forces from a simple quantum mechanical model and solved for the dynamics by an essentially exact numerical method which is tractable only at very low collision energies where few rotational levels are accessible. Subsequently Chapman and Green (1977) extended these results somewhat by using approximate

[1]Also Department of Astronomy and Space Sciences Laboratory, University of California, Berkeley.

scattering techniques. In a more recent study, Thomas, Kraemer, and Diercksen (1980) have recomputed the intermolecular forces via accurate ab initio solution of the Schrödinger equation; these authors showed that the improved potential predicted state-to-state rates which differed in some cases by up to a factor of 2 from earlier values, although the total excitation rate did not change very much. As discussed by Green and Thomas (1980), available pressure broadening data can be used to provide some check on the theory, and, in fact, agreement is within experimental error.

At high energies, where many levels are accessible, the problem becomes unwieldy due to the number of state-to-state rates which must be considered. Fortunately, when the kinetic energy is large compared to the rotational energy spacings, it can be shown that the various rates are not all independent; in particular the entire matrix of rates can be obtained simply in terms of one row γ_{J0} (Goldflam, Green, and Kouri 1977):

$$\gamma_{JJ'} = (2J'+1)\sum_L (2L+1)\begin{pmatrix} J & L & J' \\ 0 & 0 & 0 \end{pmatrix}^2 \gamma_{L0}, \quad J' < J \tag{2.1}$$

where

$$\begin{pmatrix} J & L & J' \\ 0 & 0 & 0 \end{pmatrix}$$

is the usual three-j symbol. Equation (2.1) applies only to downward rates, but upward rates can be obtained from detailed balance,

$$\gamma_{J'J} = \gamma_{JJ'}[(2J+1)/(2J'+1)] \exp(-\Delta E/kT). \tag{2.2}$$

For a given collision energy, this approximation becomes less accurate for higher rotational levels since the energy splittings increase with increasing J. As shown by DePristo *et al.* (1970), one can approximately correct for this defect by a simple modification of equation (2.1) which takes into account the rotational energy splittings:

$$\gamma_{JJ'} = (2J'+1)\sum_L (2L+1)\begin{pmatrix} J & L & J' \\ 0 & 0 & 0 \end{pmatrix}^2 A(L,J)^2 \gamma_{L0}, \quad J' < J. \tag{2.3}$$

The correction factor is given by

$$A(L,J) = [6+\Omega(L)^2]/[6+\Omega(J)^2], \tag{2.4}$$

with

$$\Omega(J') = 0.13 J' B l (\mu'/T)^{1/2}, \tag{2.5}$$

where the rotation constant B is in cm^{-1}, the collisional reduced mass μ' is in atomic mass units, the kinetic temperature T is in kelvins, and the scattering length l is in Å, with a typical value $l = 3$ Å.

The γ_{L0} needed in equation (2.3) have been obtained from new scattering calculations. Using the accurate intermolecular forces of Thomas, Kraemer, and Diercksen (1980), we computed cross sections at eleven collision energies ranging from 100 to 5000 cm^{-1} using the IOS (infinite order sudden) scattering approximation, which has been shown to be accurate for this system (see Goldflam, Green, and Kouri 1977 and Green 1979). Rate constants γ_{L0} for $L \leq 32$ were obtained by averaging these cross sections over Boltzmann distributions of collision energies at the appropriate temperatures. The resulting values, which are given in Table 1, were then used with equation (2.3) to provide all the necessary collisional rates. (Note that γ_{L0} with $L > 32$ were set to zero.)

It should be noted, finally, that all of these calculations have specifically treated excitation of CO by collisions with He atoms. It has been argued (e.g., Green and Thaddeus 1976) that excitation by H_2 is quite similar, the main difference being the greater velocity of H_2 at a given temperature due to its smaller mass. This factor will increase the rates for H_2 excitation by about 37% from the values for He. Experimental evidence in support of this procedure can be found in available pressure broadening data (Nerf and Sonnenberg 1975; see also Bréchignac *et al.* 1980).

The population of each rotational state can now be calculated from the collisional rates $\gamma_{JJ'}$ by solving the equations of statistical equilibrium for these states. In the case of CO, we can make certain simplifications which should apply interstellar shocks:

1. Each line is optically thin (cf. §§ III, IV).
2. Infrared pumping by dust emission is negligible.
3. Only the ground vibrational state contains a significant population.

Support for these assumptions can be found in observations of the Orion-KL shocked region. The far-infrared CO lines from this region have been shown to be optically thin (Watson *et al.* 1980). Furthermore, the infrared continuum data (e.g., Werner *et al.* 1976; Downes *et al.* 1981) indicate that the continuum luminosity overlapping the rotational CO lines or the fundamental vibrational band of CO at 4.6 μm is too small by several orders of magnitude to provide significant rotational or vibrational pumping. Finally, the density in Orion-KL is too small by a large factor to collisionally populate the vibrationally excited states of CO; densities of atomic hydrogen $n(H)$ in excess of 10^{10} cm^{-3} or molecular hydrogen $n(H_2)$ in excess of 10^{12} cm^{-3} are required to bring the population of the first vibrational state close to its LTE value (Scoville, Krotkov, and Wang 1980). We restrict ourselves to lower densities.

TABLE 1

He-CO Collisional Rate Coefficients[a]

γ_{L0} (cm^3 s^{-1})

L	100 K	250 K	500 K	750 K	1000 K	1500 K	2000 K
1 ...	1.72(−11)	2.31(−11)	2.53(−11)	2.65(−11)	2.75(−11)	2.92(−11)	3.07(−11)
2 ...	6.89(−12)	1.28(−11)	1.74(−11)	2.00(−11)	2.19(−11)	2.49(−11)	2.72(−11)
3 ...	4.72(−12)	7.35(−12)	8.78(−12)	9.43(−12)	9.86(−12)	1.05(−11)	1.10(−11)
4 ...	1.47(−12)	2.89(−12)	4.56(−12)	5.61(−12)	6.33(−12)	7.31(−12)	7.97(−12)
5 ...	1.54(−12)	3.07(−12)	4.38(−12)	5.07(−12)	5.51(−12)	6.06(−12)	6.40(−12)
6 ...	7.29(−13)	1.32(−12)	1.92(−12)	2.39(−12)	2.76(−12)	3.28(−12)	3.63(−12)
7 ...	4.26(−13)	1.15(−12)	2.04(−12)	2.65(−12)	3.07(−12)	3.61(−12)	3.94(−12)
8 ...	2.60(−13)	6.52(−13)	9.83(−13)	1.22(−12)	1.41(−12)	1.71(−12)	1.92(−12)
9 ...	1.27(−13)	4.87(−13)	1.00(−12)	1.42(−12)	1.76(−12)	2.24(−12)	2.55(−12)
10 ...	7.81(−14)	3.22(−13)	5.76(−13)	7.34(−13)	8.55(−13)	1.04(−12)	1.18(−12)
11 ...	3.99(−14)	2.34(−13)	5.27(−13)	7.83(−13)	1.01(−12)	1.38(−12)	1.65(−12)
12 ...	2.25(−14)	1.56(−13)	3.49(−13)	4.79(−13)	5.76(−13)	7.16(−13)	8.12(−13)
13 ...	1.19(−14)	1.12(−13)	2.92(−13)	4.43(−13)	5.84(−13)	8.38(−13)	1.05(−12)
14 ...	6.20(−15)	7.16(−14)	2.09(−13)	3.17(−13)	4.01(−13)	5.26(−13)	6.13(−13)
15 ...	3.27(−15)	5.08(−14)	1.67(−13)	2.66(−13)	3.54(−13)	5.16(−13)	6.63(−13)
16 ...	1.66(−15)	3.18(−14)	1.23(−13)	2.08(−13)	2.79(−13)	3.89(−13)	4.73(−13)
17 ...	8.14(−16)	2.15(−14)	9.56(−14)	1.67(−13)	2.28(−13)	3.37(−13)	4.33(−13)
18 ...	3.81(−16)	1.35(−14)	7.08(−14)	1.33(−13)	1.87(−13)	2.77(−13)	3.51(−13)
19 ...	1.81(−16)	8.82(−15)	5.33(−14)	1.03(−13)	1.47(−13)	2.21(−13)	2.84(−13)
20 ...	9.09(−17)	5.51(−15)	3.98(−14)	8.39(−14)	1.26(−13)	1.99(−13)	2.62(−13)
21 ...	3.84(−17)	3.34(−15)	2.86(−14)	6.38(−14)	9.76(−14)	1.54(−13)	2.00(−13)
22 ...	2.55(−17)	2.12(−15)	2.15(−14)	5.21(−14)	8.41(−14)	1.42(−13)	1.92(−13)
23 ...	5.74(−18)	1.31(−15)	1.62(−14)	4.15(−14)	6.75(−14)	1.11(−13)	1.41(−13)
24 ...	1.13(−18)	7.24(−16)	1.15(−14)	3.26(−14)	5.68(−14)	1.03(−13)	1.43(−13)
25 ...	1.52(−19)	3.86(−16)	8.29(−15)	2.52(−14)	4.47(−14)	7.97(−14)	1.06(−13)
26 ...	8.52(−20)	2.47(−16)	6.10(−15)	1.98(−14)	3.68(−14)	7.03(−14)	9.95(−14)
27 ...	4.83(−20)	1.54(−16)	4.31(−15)	1.50(−14)	2.88(−14)	5.69(−14)	8.17(−14)
28 ...	2.14(−20)	9.10(−17)	3.09(−15)	1.16(−14)	2.34(−14)	4.87(−14)	7.19(−14)
29 ...	1.35(−20)	5.80(−17)	2.18(−15)	8.85(−15)	1.89(−14)	4.24(−14)	6.54(−14)
30 ...	6.76(−21)	3.51(−17)	1.57(−15)	6.94(−15)	1.54(−14)	3.60(−14)	5.62(−14)
31 ...	8.99(−22)	1.86(−17)	1.12(−15)	5.49(−15)	1.27(−14)	3.00(−14)	4.59(−14)
32 ...	4.54(−22)	1.09(−17)	7.96(−16)	4.37(−15)	1.10(−14)	2.94(−14)	4.93(−14)

[a]Rate coefficients for He-CO collisions are given. H_2-CO rate coefficients are obtained by multiplying values in this table by 1.37.

The equations of statistical equilibrium are set up as follows. In steady state, the rate at which molecules leave each state is equal to the rate at which they enter it:

$$n_J\left[A_J + n(\mathrm{H_2})\sum_{J'}\gamma_{JJ'}\right] - \left[n(\mathrm{H_2})\sum_{J'}\gamma_{J'J}n_{J'} + n_{J+1}A_{J+1}\right] = 0, \quad (2.6)$$

where n_J is the density of molecules in state J, $n(\mathrm{H_2})$ is the density of H_2 molecules, and A_J is the A-coefficient for a radiative transition from state J to $J-1$. There is one such equation for each rotational state J. Together with the normalizing condition, $\Sigma_J n_J = n(\mathrm{CO})$, these expressions make up a complete set of linearly independent equations, the solution of which is straightforward.

In the optically thin case the line emission coefficient I_J for the transition J to $J-1$ is given by:

$$I_J = \frac{h\nu}{4\pi}\frac{A_J n_J}{n(\mathrm{CO})} \text{ ergs s}^{-1}\text{ molecule}^{-1}\text{ sr}^{-1}, \quad (2.7)$$

where ν, the transition frequency, is just $2J$ times the rotational constant B (neglecting centrifugal distortion). Figure 1 shows the line emission coefficients as a function of J for $J \leq 50$, at several temperatures and densities. These curves result from computer solution of the equations (2.6) with $J \leq 60$, as described above.

III. ANALYTIC ESTIMATE OF POPULATIONS

In order to make progress in obtaining an analytic estimate of the level populations of the CO molecule, it is necessary to make a drastic simplification in the collision cross sections $\sigma_{JJ'}$ connecting levels J and J'.

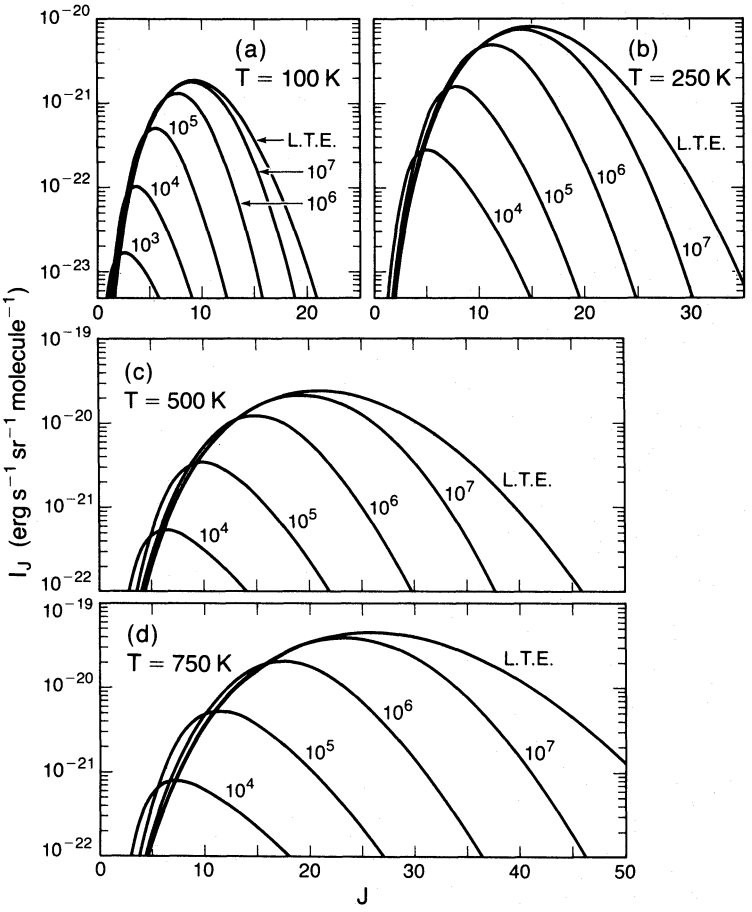

FIG. 1.—Line emission coefficient I_J for the CO rotational transitions $J \rightarrow J-1$, as a function of J for several temperatures and molecular hydrogen densities $n(H_2)$. The I_J distributions come from computer solutions of the statistical equilibrium equations, as discussed in § II. Also shown, for comparison, are the I_J distributions resulting from thermal equilibrium (LTE) level populations.

Here we follow HM and adopt

$$\gamma_{JJ'} = \langle \sigma_{JJ'} v \rangle = \frac{g_{J'} \exp(-E_{J'}/kT) \sigma v_T}{Z}, \quad (3.1)$$

where Z is the partition function, $v_T = [8kT/\pi m(H_2)]^{1/2}$ is the mean speed of the H_2 molecules, $g_{J'} = 2J'+1$ is the degeneracy of the state J', and σ is the total collision cross section out of level J:

$$\sum_{J'=0}^{\infty} \langle \sigma_{JJ'} v \rangle = \sigma v_T. \quad (3.2)$$

Equation (3.1) for the cross section has the advantages that it satisfies detailed balance and it facilitates solution of the level population equations. Its major disadvantage is that it depends only on the final state and therefore omits a conspicuous feature of the calculated cross sections, namely that collisions with small ΔJ are strongly favored over those with large ΔJ (cf. Table 1). Numerical evaluation of σ shows that it is about 10^{-15} cm^2, as assumed by HM; the effective value required to determine the level population is smaller, as we shall see below. With expression (3.1) for the cross section, equation (2.3) for the level populations readily simplifies to

$$n_J\left(A_J + \tfrac{1}{2} n \sigma v_T\right) = n_{J+1} A_{J+1} + \tfrac{1}{2} n n_J^* \sigma v_T, \quad (3.3)$$

where

$$n_J^* = n(\mathrm{CO}) \frac{g_J e^{-E_J/kT}}{Z} \quad (3.4)$$

is the LTE population, n is the number density of hydrogen nuclei, and $n(H_2) = n/2$ in a fully molecular gas. In deriving equation (3.3), we set $\sigma_{JJ} = 0$ and took $n_J \ll n(\mathrm{CO})$. Although in this paper we are focusing on the case of optically thin emission, it is a simple matter to include the effects of line opacity via the escape probability formalism (e.g., de Jong 1973; HM). If $\varepsilon_J \leq 1$ is the probability that a photon in the $J \rightarrow J-1$ transition can escape the emission region, then the transition

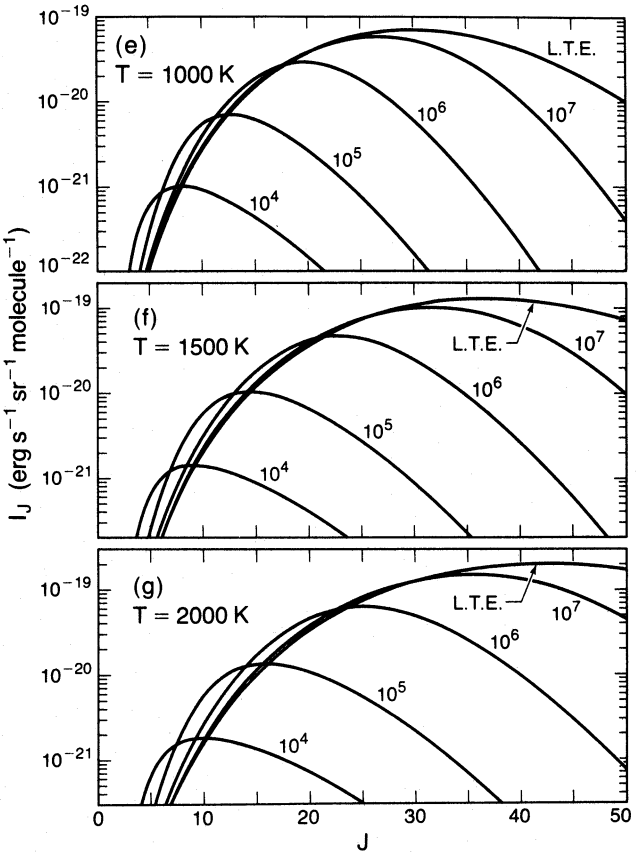

FIG. 1.—*Continued*

probability A_J is replaced by $A_J\varepsilon_J$ in equation (3.3). Making this substitution, we introduce

$$a_J \equiv \frac{2A_J\varepsilon_J}{n\sigma v_T}. \tag{3.5}$$

Then, in terms of the departure coefficients $b_J = n_J/n_J^*$, the population equation becomes

$$b_J(a_J+1) = b_{J+1}a_{J+1}\frac{n_{J+1}^*}{n_J^*} + 1 \tag{3.6}$$

which has the solution

$$a_J b_J = \sum_{J'=J}^{\infty} \frac{n_{J'}^*}{n_J^*} \prod_{J''=J}^{J'} \frac{a_{J''}}{1+a_{J''}} \quad (J \geq 1). \tag{3.7}$$

The ground state population is then given by

$$b_0 = b_1 a_1 \frac{n_1^*}{n_0^*} + 1 \quad (J=0). \tag{3.8}$$

In view of the approximate form of the cross section used in obtaining the solution (3.7), considerable simplification is warranted. For simplicity, assume $J \gg 1$ so that

$$A_J \approx A_0 J^3, \quad E_J \approx E_0 J^2, \tag{3.9}$$

where, for CO, $A_0 = 1.118\times10^{-7}$ s^{-1} and $E_0/k = 2.765$ K. Define y and J_T by:

$$y \equiv \frac{E_J}{kT} = \frac{E_0 J^2}{kT} \equiv \frac{J^2}{J_T^2}. \tag{3.10}$$

For $kT \gg E_0$, the partition function is simply $Z = J_T^2$. The energy difference ΔE_J between levels J and $J-1$ is about $2E_0 J$ so that

$$\Delta E_J/kT \approx 2y/J. \tag{3.11}$$

The quantity a_J defined in equation (3.5) can be

expressed

$$a_J = \frac{J}{4} y \frac{n_{cr}}{n} \varepsilon_J, \tag{3.12}$$

where

$$n_{cr} \equiv 8 \frac{J_T^2 A_0}{\sigma v_T} \tag{3.13}$$

is the density of hydrogen nuclei at which collisional de-excitation becomes important in an optically thin gas (HM).

First, consider the high density limit in which $a_J \to 0$ and the levels are nearly in LTE. Treating both a_J and J^{-1} as small and keeping terms to second order in small quantities, we find that the solution (3.7) reduces to

$$b_J \approx \frac{1+(n_{cr}\varepsilon_J/n)y}{1+\frac{1}{2}(n_{cr}\varepsilon_J/n)y^2}. \tag{3.14}$$

In the opposite, low density limit, $a_J \to \infty$ and we find for either $J \gg 1$ or $J = 0$

$$b_J \approx \left[b_0^{-1} + \tfrac{1}{2}(n_{cr}\varepsilon_J/n)y^2\right]^{-1}. \tag{3.15}$$

There is considerable latitude in combining equations (3.14) and (3.15) into a general approximation for all densities. Since the quantum mechanical calculation of the cross sections shows that σ decreases slowly with J, we expect that n_{cr} will increase slowly with y. Hence we make the replacement

$$\frac{n_{cr}\varepsilon_J}{n} \to w y^{\beta} \tag{3.16}$$

and treat w and β as parameters to be determined by comparison with the numerical results for the level populations presented in § II. Using expressions (3.14) and (3.15) as a. foundation, we have developed the following approximation for the departure coefficients in the optically thin case by trial-and-error comparison with the detailed numerical results:

$$b_J = \frac{1+wy^{1.3}}{b_0^{-1} + \frac{1}{2}wy^{2.3}(1+wy^{1.3})}(f_1 f_2)^{-1} \tag{3.17}$$

$$b_0 = \left(1+\tfrac{2}{3}w^{0.83}\right)^{1/2}, \tag{3.18}$$

where

$$f_1 = \left(1 + \frac{0.55y^{2.2}}{T_3^{-0.2} + 8w^{-0.75}}\right)^2 \tag{3.19}$$

$$w = \frac{2.75T_3^{\alpha}}{n_6} = \frac{1.38T_3^{\alpha}}{n(\mathrm{H}_2)_6} \tag{3.20}$$

$$\alpha = 0.74 + 0.16T_3^{1/2} \tag{3.21}$$

and

$$f_2 = (f_a/f_b)^{(T_3/3)^{1.1}} \tag{3.22}$$

$$f_a = 1 + \frac{0.2(w/T_3)^{0.6}}{1+0.1w} + \frac{0.32(wy^{2.3})^{(T_3/3)^{0.3}}}{1+T_3} \tag{3.23}$$

$$f_b = \left(1+0.9w^{1.3}y^{2.3}\right)^{0.32} \tag{3.24}$$

with $n_6 \equiv n/(10^6\ \mathrm{cm}^{-3})$ and $T_3 \equiv T/(10^3\ \mathrm{K})$. The primary effect of the factor $f_1 f_2$ is to reduce the populations at large values of J, thereby accounting for the inefficiency of collisions with large ΔJ; for $y < \frac{1}{2}$ and $n > 2\times 10^4\ \mathrm{cm}^{-3}$, $f_1 f_2$ is within a factor of 2 of unity.

This analytic approximation is remarkably accurate over a wide range of physical conditions. Let J_p be the rotational quantum number of the highest level which produces a line with an intensity within a factor of 50 of the strongest line; if the strongest line is at J_m, then typically $J_p \sim 2J_m$. Comparison with the numerical results shows that our approximation is correct to within a factor 1.34 for $0 \le J \le J_p \le 57$ over the range $n \ge 2\times 10^4\ \mathrm{cm}^{-3}$ and $250\ \mathrm{K} \le T \le 3000\ \mathrm{K}$, a somewhat broader range than covered by Figure 1. At $T = 100$ K, this accuracy is achieved only for $n \gtrsim 5\times 10^4\ \mathrm{cm}^{-3}$. The accuracy is degraded at lower densities: omitting low lying levels which produce lines with an intensity less than 2% of the strongest lines (i.e., $J = 0$ and sometimes $J = 1$), then the accuracy is better than a factor of 1.5 for $100\ \mathrm{K} \le T \le 1500$ at $n = 2\times 10^3\ \mathrm{cm}^{-3}$; it becomes worse at higher temperatures.

As indicated above, the approximation developed here can be readily extended to the case of finite optical depth in the lines by multiplying the value of w given in equation (3.20) by the escape probability ε_J. We have not attempted to assess the accuracy of this procedure, however.

IV. POPULATION INVERSION

Population inversions result in maser action and can produce extremely intense sources of radiation. Because of high abundance of CO in molecular clouds, inversion of CO levels could be particularly important. Goldsmith (1972) suggested that the $J = 1$ level of CO could become inverted because collisions from $J = 0$ to $J = 2$ occur at a rate comparable to those from $J = 0$ to $J = 1$,

TABLE 2

POPULATION INVERSIONS AND "SATURATION" COLUMN DENSITIES FOR CO

T(K)	$J=1$		$J=2$		$J=3$		$J=4$	$J=5$	$J=6$	$J=7$
$n(H_2)$[a]	10^4	10^5	10^4	10^5	10^4	10^5	10^5	10^5	10^5	10^5
100	1.21[b]	...	...	...	...	...	...	...	...	...
	1.41(16)[b]	...	...	...	...	...	...	...	...	...
250	1/257	1.002	1.043	...	...	...	...	...	...	...
	3.79(16)	1.09(19)	8.93(16)	...	...	...	...	...	...	...
500	1.221	1.007	1.228	1.012	...	1.014	1.001			
	1.03(17)	7.86(18)	4.08(16)	2.06(18)	...	1.19(18)	1.10(19)	...	...	...
750	1.194	1.008	1.286	1.015	1.001	1.021	1.021	1.004	...	...
	1.91(17)	1.15(19)	5.4(16)	2.85(18)	1.10(19)	1.32(18)	9.73(17)	4.59(18)	...	...
1000	1.174	1.008	1.307	1.016	1.086	1.023	1.028	1.022	...	...
	3.00(17)	1.60(19)	7.24(16)	3.91(18)	1.32(17)	1.73(18)	1.06(18)	1.05(18)	...	...
1500	1.147	1.008	1.308	1.016	1.187	1.024	1.031	1.035	1.026	...
	5.69(17)	2.69(19)	1.18(17)	6.47(18)	9.94(16)	2.34(18)	1.55(18)	1.09(18)	1.17(18)	...
2000	1.130	1.007	1.295	1.015	1.240	1.023	1.032	1.038	1.037	1.022
	8.86(17)	3.88(19)	1.73(17)	9.36(18)	1.09(17)	4.01(18)	2.17(18)	1.40(18)	1.15(18)	1.62(18)

[a] Value of $n(H_2)$ in cm^{-3}.

[b] The upper entry for each $[T, n(H_2), J]$ is the population inversion $n_J g_{J-1}/n_{J-1} g_J$; the lower is the saturation column density N_{sat} in cm^{-2}.

whereas radiative transitions from $J=2$ to $J=1$ occur much more rapidly than from $J=1$ to $J=0$. In a detailed calculation including radiative transfer, Leung and Liszt (1976) found that at 40 K the $1\rightarrow 0$ transition became suprathermal (excitation temperature > kinetic temperature) but not inverted. Because of the lower optical depth in ^{13}CO, much higher excitation temperatures were achieved in ^{13}CO than in ^{12}CO. Actual inversions were predicted in the CS molecule at this temperature (Liszt and Leung 1977). Calculations of the populations in cyanoacetylene (HC_3N), which is a linear molecule like CO, indicate that the $1\rightarrow 0$ transition can be inverted for $10^3\ cm^{-3} \lesssim n \lesssim 10^5\ cm^{-3}$, whereas the $2\rightarrow 1$ transition is inverted over a narrower range (Morris *et al.* 1976). The latter authors claimed evidence for a weak cyanoacetylene maser in Sgr B2.

Using the detailed numerical calculations discussed in § II, we have made a systematic search for population inversions in CO over a wide range of temperatures and densities. We have not included any radiative transfer effects, because that would entail making additional assumptions about the geometry of the source and the intensity of the background radiation. We find that the $1\rightarrow 0$ transition can be inverted for $T \approx 50$ K over a narrow range of densities; as the temperature is increased, the range of densities over which an inversion occurs increases and higher levels become inverted as well. The mechanism for producing the inversions is a direct generalization of that suggested by Goldsmith (1972): collisional rates vary more slowly with J than do the radiative rates, so it is possible for molecules to become trapped at high J.

Our results are summarized in Table 2 and Figure 2. The magnitude of the inversion $n_J g_J^{-1}/(n_{J-1} g_{J-1}^{-1})$ and the "saturation column density" N_{sat} are presented as a function of J, $n(H_2)$, and T. When the CO column density equals N_{sat}, the optical depth in the $J\rightarrow J-1$ transition is -1. For $N(CO) < N_{sat}$, our optically thin approximation is valid, but the amplification is small. For $N(CO) > N_{sat}$, the amplification could be large in principle, but a detailed radiative transfer calculation would be needed to make certain. The value of N_{sat} is determined by the optical depth τ_J in the $J\rightarrow J-1$

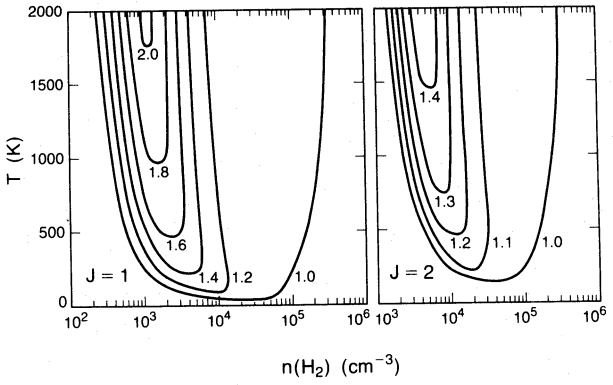

FIG. 2.—Population inversion $n_J g_{J-1}/n_{J-1} g_J$ as a function of temperature and molecular hydrogen density for the $J=1$ and $J=2$ states of CO. These curves were generated using computer solutions of the statistical equilibrium equations, as discussed in § II.

transition. At the center of a Gaussian line we have

$$\tau_J = N_{J-1}\frac{g_J}{g_{J-1}}\frac{\lambda^3 A_J}{8\pi^{3/2}\Delta v}\left(1-\frac{N_J g_{J-1}}{N_{J-1}g_J}\right) \quad (4.1)$$

where N_J is the column density in level J. The line width Δv is taken to be the half width to e^{-1} points of the line, expressed in velocity units; for a thermal profile, CO lines have $\Delta v = (T/1680)^{1/2}$ km s^{-1}. If the line profile is dominated by systematic motions, then $N_{J-1}/\pi^{1/2}\Delta v$ should be replaced by $dN_{J-1}/dv = n_{J-1}(dv/dr)^{-1}$. Noting that $A_J \propto \mu^2\lambda^{-3}$, where μ is the dipole moment, we can solve equation (4.1) for N(CO) when $\tau = -1$ and obtain

$$N_{\rm sat} = 1.12\times 10^{15}\left[\frac{N_{J-1}}{N(\rm CO)}\frac{J}{(2J-1)(\Delta v)_5}\right.$$
$$\left.\times\left(\frac{N_J g_{J-1}}{N_{J-1}g_J}-1\right)\right]^{-1} \text{ cm}^{-2}, \quad (4.2)$$

where the ratios N_{J-1}/N(CO) and N_J/N_{J-1} may be obtained from the calculations described in § II and $(\Delta v)_5 = \Delta v/(10^5$ cm s$^{-1})$. The values for $N_{\rm sat}$ given in Table 2 are minimum values because we adopted the minimum line width—the thermal width. CO has unusually large values of $N_{\rm sat}$ because of its small dipole moment.

The conditions required for a population inversion may be understood as follows. Let J_l be the level at which n_J is a maximum; obviously, an inversion is possible only for $J < J_l$. If the density is too high, then the populations approach their LTE values, and no inversion is possible. If either the density or the temperature is too low, then J_l will drop below J, and again no inversion is possible for level J. The upper limit on the density can be estimated from the approximation developed in § III; unfortunately, the lower limit occurs at a density too low for the approximation to be valid. Since an inversion is possible only for low values of J, the quantity $y = J^2/J_T^2$ is small, and the factor $f_1 f_2$ can be set equal to unity in equation (3.17). Hence b_J depends only on the two variables w and y, and not on n, T, and J separately. The condition that an inversion occur for a specified y can then depend only on w. Since an inversion is possible only for densities below some critical value (which depends on T), the condition must be a lower limit on w; i.e., we require $w > w_{\rm crit}$ for an inversion. Inspection of Table 2 suggests $w_{\rm crit} \approx 4$, which gives

$$n(\rm H_2) \lesssim 10^{5.5} T_3^{\alpha} \text{ cm}^{-3} \quad (4.3)$$

as the condition for an inversion. At $T \approx 50$ K, the upper and lower limits on the density converge at $n(\rm H_2) \sim 3\times 10^4$ cm^{-3}; the numerical calculations show that an inversion is impossible for $T \lesssim 50$ K. As T increases above 50 K, J_l rises so that higher levels become inverted as well.

As emphasized above, our calculation of population inversions is valid only in the optically thin limit, $N < N_{\rm sat}$, which seemingly precludes large amplifications. However, if the CO is in a thin sheet, then our calculations may be directly applicable even if the amplification is large: in most directions one could have N(CO) $< N_{\rm sat}$ so that the level populations are unaffected by radiative transfer, but when viewed edge-on, the sheet could have N(CO) $\gg N_{\rm sat}$, producing a source of high brightness. (However, only a limited amplification would be possible before the level populations would be affected.) Such conditions are expected for interstellar shocks. Observations of regions containing interstellar shocks, with sufficient spatial resolution to resolve the shock thickness, could reveal regions of anomalously high brightness in the lower CO rotational lines. A possible example of such a region is IC 443 (De Noyer 1979*a*, *b*) where some components may be edge-on, although the excitation seems too small to produce inversion. Unfortunately, in Orion, the best studied example of interstellar molecular shocks, the observed CO emission originates in gas which is too dense [$n(\rm H_2) \sim 10^5 - 10^6$ cm^{-3}] to produce a significant population inversion.

Detailed calculations are required to determine if significant amplification can occur in actual interstellar shocks. Reference to Table 2 shows that relatively large column densities of warm gas are required to produce one *e*-folding in the intensity: $N(\rm H) \approx 10^{20-21}$ cm^{-2} at $n(\rm H_2) = 10^4$ cm^{-3} and $N(\rm H) \approx 10^{21.5-22.5}$ cm^{-2} at $n(\rm H_2) = 10^5$ cm^{-3}, under the assumption that $n(\rm CO)/n \approx 10^{-4}$. If the emission occurs in a magnetic precursor to the shock or in a *C*-type shock (Draine 1980) then n is the preshock density; if the emission occurs in the shocked gas, then n is the shocked density, which is typically 10–30 times greater (HM). In a *C*-type shock, the velocity width of the emission in the direction of the shock velocity can be comparable to the shock velocity itself. This increases $N_{\rm sat}$ in that direction and ensures that the emission is optically thin. In the perpendicular direction (i.e., in the plane of the shock), the velocity width is of order the thermal velocity, which facilitates building up optical depths $|\tau| > 1$ in a narrow range of directions. On the other hand, in a conventional shock, the velocity width is predominantly thermal everywhere behind the shock front for $\rm H_2$ and for $T < 0.5\ T_s$ for CO, where T_s is the postshock temperature.

V. OPTICALLY THIN COOLING RATES

Because of its relatively high abundance, CO is often an important coolant in molecular clouds (e.g., Dalgarno *et al.* 1975). We define the rotational cooling rate coeffi-

cient $L_{\rm rot}$ by setting $n \cdot n({\rm CO}) \cdot L_{\rm rot}$ equal to the total CO rotational emission rate; assuming that the gas is optically thin, we have

$$n \cdot n({\rm CO}) \cdot L_{\rm rot} = \sum_{J=1}^{\infty} n_J A_J \Delta E_J = 4\pi n({\rm CO}) \sum_{J=1}^{\infty} I_J, \tag{5.1}$$

where ΔE_J is the energy difference between levels J and $J-1$, and I_J is defined in equation (2.7). HM obtained the approximate result

$$L_{\rm rot} = \frac{4(kT)^2 A_0}{nE_0\left[1+(n_{\rm cr}/n)+1.5(n_{\rm cr}/n)^{1/2}\right]} \tag{5.2a}$$

$$= \frac{\frac{1}{2}kT\sigma v_T}{1+(n/n_{\rm cr})+1.5(n/n_{\rm cr})^{1/2}}, \tag{5.2b}$$

where the equivalence of the two expressions follows from the definition of $n_{\rm cr}$, equation (3.13). The factor $\frac{1}{2}$ in equation (5.2b) is simply $n({\rm H}_2)/n$.

Using the numerical results discussed in § II, we find that this expression is remarkably accurate—i.e., to within 20%—for 2×10^3 cm$^{-3} < n < 2\times10^7$ cm^{-3} and 250 K $< T <$ 3000 K if we set

$$n_{\rm cr} = 3.3\times10^6 T_3^{3/4}\ {\rm cm}^{-3}, \tag{5.3}$$

which corresponds to

$$\sigma = 3.0\times10^{-16} T_3^{-1/4}\ {\rm cm}^{-2}. \tag{5.4}$$

At higher densities equations (5.3) and (5.4) are less accurate, but the cooling is sufficiently close to its LTE value that this does not matter. At lower temperatures, these equations are also less accurate; at $T = (100$ K, 50 K, 30 K), $L_{\rm rot}$ is accurate to within a factor (1.3, 1.6, 2) for $n > 2\times10^3$ cm^{-3}. Numerically, the rotational cooling rates of optically thin CO in a fully molecular gas is

$$nn({\rm CO})L_{\rm rot} = \begin{cases} 8.3\times10^{-21} T_3^2 \left[\dfrac{x({\rm CO})}{3.7\times10^{-4}}\right] n\ {\rm ergs\ cm^{-3}\ s^{-1}} & (5.5a) \\ 2.5\times10^{-27} T_3^{5/4} \left[\dfrac{x({\rm CO})}{3.7\times10^{-4}}\right] n^2\ {\rm ergs\ cm^{-3}\ s^{-1}} & (5.2b) \end{cases}$$

at high ($n \gg n_{\rm cr}$) and low ($n \ll n_{\rm cr}$) densities, respectively, where $x({\rm CO})/3.7\times10^{-4}$ is the abundance of CO normalized to the cosmic abundance of carbon. Note that equation (5.5) is valid only for warm molecular gas, $T \gtrsim 150$ K.

Comparison of these results with those of HM shows that their estimate of the low density cooling is too high by about a factor of 3 (if eq. [5.2b] is used), and their estimate of $n_{\rm cr}$ is too low by a factor of 5. The difference is due to the fact that they set $\sigma = 10^{-15}$ cm^2 and that they used a thermal velocity appropriate for atomic hydrogen. A similar reduction in the low-density rotational cooling of the other dipolar molecules considered by HM also may be in order. Calculations by T. Takahashi (1981, private communication) show that the effective cooling cross section σ for H_2O is 3×10^{-16} cm^2, at least for 100 K $\lesssim T \lesssim$ 500 K; the corresponding value of $n_{\rm cr}$ is $1.1\times10^{11} T_3^{1/2}$ cm^{-3}, again about 5 times the HM value.

How does CO rotational velocity cooling compare with other coolants in warm molecular gas?

a) Other dipolar molecules.—Equation (5.5) applies approximately to other dipolar molecules such as H_2O if $x({\rm CO})$ is replaced by $x(H_2O)$, etc. Hence, in low density [$n < n_{\rm cr}({\rm CO})$], optically thin gas, CO will always be significant because it is one of the most abundant dipolar molecules. Because of the small dipole moment of CO, its critical density is small compared to that of H_2O or OH; hence, these molecules will tend to dominate the cooling for $n > n_{\rm cr}({\rm CO})$. Since line opacity reduces the cooling only if the density is high enough for collisional de-excitation to occur, cooling by H_2O and OH, which have very large values of $n_{\rm cr}$, will also tend to dominate that due to CO in opaque regions.

b) Molecular hydrogen.—CO cooling dominates rotational-vibrational cooling by H_2 at high densities and low temperatures. For $n \gg n_{\rm cr}({\rm CO})$, comparison with HM's cooling rates for H_2 shows that CO dominates at $T = 1000$ K provided $x({\rm CO}) \gtrsim 6\times10^{-5}$; at $T = 3000$ K, CO cooling is as large as H_2 cooling only if all the carbon is in CO. At lower temperatures, CO dominates H_2 over a wide range of densities. For example, at $T = 300$ K, CO cooling exceeds H_2 cooling for $n > 5000[3.7\times10^{-4}/x({\rm CO})]$ cm^{-3}.

c) Grain cooling.—Dominates CO rotational cooling at high densities, $n \gtrsim 2\times10^9 T_3^{1/2}[x({\rm CO})/3.7\times10^{-4}]$ cm^{-3}, for standard grain parameters (cf. HM), provided $T_{\rm grain} \lesssim \frac{1}{2}T$.

d) CO vibrational cooling.—Becomes important at high temperatures and densities provided there is a substantial fraction of atomic hydrogen (Scoville *et al.* 1980). However, in a fully molecular gas [$n({\rm H})/n \lesssim 0.01$], H_2 cooling and grain cooling almost always exceed CO vibrational cooling (HM). In a fully molecular gas, a sufficient condition for CO rotational cooling to dominate CO vibrational cooling is $n < 2\times10^8$ cm^{-3} and $T < 4000$ K. If the vibrational excitation is determined by H atoms, this condition is $n({\rm H}) < 2\times10^6$ cm^{-3} and $T < 4000$ K.

Note that equation (5.5) applies only in a gas of molecular hydrogen. Behind fast shocks, relatively large concentrations of atomic hydrogen can build up (Hollenbach and McKee 1980). If $x_2 = n(H_2)/n$, then in the presence of atomic hydrogen, the critical density (eq. [3.14]) becomes

$$n_{cr} = \frac{4J_T^2 A_0}{\sigma v_T [x_2 + (\sigma_H/\sigma)(1-2x_2)2^{1/2}]}, \quad (5.7)$$

where σ_H is the effective cross section for rotational excitation in collisions of atomic hydrogen with CO. In a fully molecular gas, $x_2 = 1/2$, and equation (3.14) is recovered.

VI. CONCLUSION

The numerical and analytic results we have presented for the rotational spectrum of CO should be useful in interpreting observations of interstellar CO emission from warm molecular gas and in generating theoretical models of shocks in molecular clouds. The results are valid for optically thin CO which is collisionally excited by H_2 collisions; infrared pumping has been ignored. The analytic results can be extended to the optically thick case in an approximate fashion by using the escape probability formalism.

An important result of our analysis is that in the absence of photon trapping population inversions in the lower rotational levels of CO can be expected to occur in warm molecular gas with density in the range $n(H_2) \approx 10^{3-5}$ cm^{-3}. The number of levels for which an inversion occurs and the column density required for significant amplification both increase with temperature (see Table 2). Interstellar shocks are potential sites of CO masers. Finally, the expression for the CO cooling rate obtained by HM has been verified, although we find a numerical value which is several times smaller at low densities. A similar reduction may be in order for OH and H_2O, the other dipolar molecules which are important coolants.

C. F. M. gratefully acknowledges numerous conversations with D. Hollenbach. His research is supported by NSF grant AST 79-23243. J. W. V. S. and D. M. W. are supported in part by NASA grant NGR 05-003-511. S. G. acknowledges partial support from NASA grant NSG 7105.

REFERENCES

Bréchignac, P., Picard-Bersellini, A., Charneau, R., and Launay, J. M. 1980, *Chem. Phys.*, **53**, 165.
Chapman, S., and Green, S. 1977, *J. Chem. Phys.*, **67**, 2317.
Dalgarno, A., de Jong, T., Oppenheimer, M., and Black, J. H. 1975, *Ap. J. (Letters)*, **192**, L37.
de Jong, T. 1973, *Astr. Ap.*, **26**, 297.
De Noyer, L. K. 1979 *a*, *Ap. J. (Letters)*, **228**, L41.
_____. 1979*b*, *Ap. J. (Letters)*, **232**, L165.
DePristo, A. E., Augustin, S. D., Ramaswamy, R., and Rabitz, H. 1979, *J. Chem. Phys.*, **71**, 850.
Downes, D., Genzel, R., Becklin, E. E., and Wynn-Williams, C. G. 1981, *Ap. J.*, **244**, 869.
Draine, B. 1980, *Ap. J.*, **241**, 1021.
Goldflam, R., Green, S., and Kouri, D. J. 1977, *J. Chem. Phys.*, **67**, 4149.
Goldsmith, P. F. 1972, *Ap. J.*, **176**, 597.
Green, S. 1979, *Chem. Phys.*, **40**, 1.
Green, S., and Thaddeus, P. 1976, *Ap. J.*, **205**, 766.
Green, S., and Thomas, L. D. 1980, *J. Chem. Phys.*, **73**, 5391.
Hollenbach, D. J., and McKee, C. F. 1979, *Ap. J. Suppl.*, **41**, 555 (HM).
_____. 1980, *Ap. J. (Letters)*, **241**, L47.
Leung, C. M., and Liszt, H. S. 1976, *Ap. J.*, **208**, 732.
Liszt, H. S., and Leung, C. M. 1977, *Ap. J.*, **218**, 396.
Morris, M., Turner, B. E., Palmer, P., and Zuckerman, B. 1976, *Ap. J.*, **205**, 82.
Nerf, R. B., and Sonnenberg, M. A. 1975, *J. Molec. Spectrosc.*, **58**, 474.
Scoville, N. Z., Krotkov, R., and Wang, D. 1980, *Ap. J.*, **240**, 929.
Storey, J. W. V., Watson, D. M., Townes, C. H., Haller, E. E., and Hansen, W. L. 1981, *Ap. J.*, **247**, 136.
Thomas, L. D., Kraemer, W. P., and Diercksen, G. H. F. 1980, *Chem. Phys.*, **51**, 131.
Watson, D. M., Storey, J. W. V., Townes, C. H., Haller, E. E. and Hansen, W. L. 1980, *Ap. J. (Letters)*, **239**, L129.
Werner, M. W., Gatley, I., Harper, D. A., Becklin, E. E., Loewenstein, R. F., Telesco, C. M., and Thronsen, H. A. 1976, *Ap. J.*, **204**, 420.

SHELDON GREEN: NASA Institute for Space Studies, 2880 Broadway, New York, NY 10025

CHRISTOPHER F. McKEE and DAN M. WATSON: Department of Physics, University of California, Berkeley, CA 94720

J. W. V. STOREY: Anglo-Australian Observatory, P.O. Box 296, Epping, N.S.W. 2121, Australia